SECURITY CLASSIFICATION OF THIS PAGE

REPORT DOCUMENTATION PAGE

Form Approved OMB No. 0704-0188

1a. REPORT SECURITY CLASSIFICATION: Unclassified	1b. RESTRICTIVE MARKINGS
2a. SECURITY CLASSIFICATION AUTHORITY	3. DISTRIBUTION/AVAILABILITY OF REPORT: Approved for public release. Distribution is unlimited.
2b. DECLASSIFICATION/DOWNGRADING SCHEDULE	
4. PERFORMING ORGANIZATION REPORT NUMBER(S): Technical Report No. 14	5. MONITORING ORGANIZATION REPORT NUMBER(S)
6a. NAME OF PERFORMING ORGANIZATION: Cornell University; 6b. OFFICE SYMBOL (If applicable)	7a. NAME OF MONITORING ORGANIZATION: Office of Naval Research
6c. ADDRESS (City, State, and ZIP Code): Olin Hall, Cornell University, Ithaca, NY 14853	7b. ADDRESS (City, State, and ZIP Code): 800 North Quincy Street, Arlington, VA 22217
8a. NAME OF FUNDING/SPONSORING ORGANIZATION: Office of Naval Research; 8b. OFFICE SYMBOL (If applicable)	9. PROCUREMENT INSTRUMENT IDENTIFICATION NUMBER: N 00014-85-K-0474
8c. ADDRESS (City, State, and ZIP Code)	10. SOURCE OF FUNDING NUMBERS: PROGRAM ELEMENT NO. / PROJECT NO. / TASK NO. / WORK UNIT ACCESSION NO.

11. TITLE (Include Security Classification): Quantitative Analysis of Laser Interferometer Waveforms Obtained During Oxygen Reactive-Ion Etching of Thin Polymer Films

12. PERSONAL AUTHOR(S): B. C. Dems, P. D. Krasicky, and F. Rodriguez

13a. TYPE OF REPORT	13b. TIME COVERED	14. DATE OF REPORT (Year, Month, Day)	15. PAGE COUNT
Technical Report	FROM _____ TO _____	89 May 12	20

16. SUPPLEMENTARY NOTATION: Prepared for presentation before the ACS Div. of Polymeric Materials:Science & Engineering, Symp. on Polymers in Microlithography, Dallas, TX, April 9-14, 1989

17. COSATI CODES		
FIELD	GROUP	SUB-GROUP

18. SUBJECT TERMS (Continue on reverse if necessary and identify by block number): Laser Interferometer, Reactive Ion Etching, Plasma, Resist, Microlithography. (AW)

19. ABSTRACT (Continue on reverse if necessary and identify by block number)

Continuous laser interferometry, especially of inorganic materials, during reactive ion etching often has been used as an end-point detection method. However, the detailed patterns obtained during etching of thin organic polymer films have not been fully exploited. The sinusoidal oscillations in reflected light intensity often exhibit almost uniform amplitudes. In addition to variations in the rate of etching with time or depth, a rigorous analysis of the waveform yields an in situ measure of the refractive index of the film. A reduction factor for the medium/polymer interface Fresnel coefficient is used to account for the diffuseness arising from "roughening" of the film. Ion bombardment causes the roughening and necessitates the correction which is not usually the case when interferometry is used in solvent dissolution studies. The analysis, an iterative procedure for its use, and the application to oxygen/RIE of several polymers will be described. Keywords:)

Single quotes

20. DISTRIBUTION/AVAILABILITY OF ABSTRACT	21. ABSTRACT SECURITY CLASSIFICATION
☒ UNCLASSIFIED/UNLIMITED ☐ SAME AS RPT. ☐ DTIC USERS	Unclassified
22a NAME OF RESPONSIBLE INDIVIDUAL: Dr. J. Milliken	22b TELEPHONE (Include Area Code): (202) 696-4410; 22c OFFICE SYMBOL

DD Form 1473, JUN 86 — Previous editions are obsolete. — SECURITY CLASSIFICATION OF THIS PAGE

OFFICE OF NAVAL RESEARCH

Contract N00014-85-K-0474

Technical Report No. 14

QUANTITATIVE ANALYSIS OF LASER INTERFEROMETER WAVEFORMS OBTAINED DURING OXYGEN REACTIVE-ION ETCHING OF THIN POLYMER FILMS

by

B. C. Dems, P. D. Krasicky, and F. Rodriguez

Prepared for presentation before the
ACS Division of Polymeric Materials: Science and Engineering
International Symposium on Polymers in Microlithography
Dallas, TX, April 9-14, 1989

Olin Hall, Cornell University
School of Chemical Engineering
Ithaca, NY 14853

MAY 12, 1989

Quantitative Analysis of a Laser Interferometer Waveform Obtained During Oxygen Reactive-Ion Etching of Thin Polymer Films

B.C. Dems, P.D. Krasicky, and F. Rodriguez
School of Chemical Engineering, Olin Hall,
Cornell University, Ithaca, NY 14853

Laser interferometry is used extensively in the integrated circuit and thin film processing industries. It is well-suited for end-point detection and *in situ* etch rate monitoring during the plasma processing of thin polymer films. The qualitative features of the laser interferogram can also shed light on physical changes occurring at any particular time in the process. This paper describes a rigorous analysis of an interferogram which allows the polymer's refractive index to be calculated directly from the waveform. This in turn allows *in situ* etch rate determination without prior knowledge of the polymer film's physical properties. The analysis also allows the degree of surface roughening imparted to the film during plasma processing to be assessed on a relative basis. The analysis is restricted to: (a) plasma processes which have a large chemical etch component, (b) to etch gases which do not contain film-forming pre-cursors, and (c) polymer films which remain homogeneous at all times.

BACKGROUND

A model for the type of thin film system realized in Reactive-Ion Etching (RIE) is shown in figure 1. The polymer film is labeled as region #2, the substrate as #3, and the plasma environment as #1. The polymer-substrate (2-3) interface is assumed to be sharp and smooth, but the plasma-polymer (1-2) interface may be diffuse or rough. Unpolarized light of vacuum wavelength

λ is incident upon the system from region #1 at an angle ϑ_1 relative to the normal. The system's overall reflectance R is given by [1],

$$R = \frac{I}{I_o} = \left(\frac{r_{23}^2 + 2fr_{12}r_{23}\cos\phi + f^2r_{12}^2}{1 + 2fr_{12}r_{23}\cos\phi + f^2r_{12}^2r_{23}^2} \right) \qquad (1)$$

where I_o and I are the incident and reflected light intensities, respectively. The r's with subscripts are Fresnel reflection coefficients for sharp, smooth interfaces between the media denoted, while f is a reduction factor for reflection from the plasma-polymer (1-2) interface and accounts for spreading of the interface into a transition region. R is a periodic function of the film thickness d through the phase function $\phi = \phi_2 + \phi_t$, which includes the phase delay [2],

$$\phi_2 = (4\pi d/\lambda)(n_2^2 - n_1^2\sin^2\vartheta_1)^{\frac{1}{2}} \qquad (2)$$

associated with passage of light through the film to the substrate and back, as well as any additional phase shift ϕ_t introduced by the transition region. When the 1-2 interface is perfectly sharp and smooth, then f = 1, $\phi_t = 0$, and the maximum value of the periodically oscillating reflectance equals the reflectance of the bare substrate after the film is completely removed. The optical effect of $f < 1$ is a reduction in amplitude of oscillation of R from what it would be for an otherwise sharp, smooth interface.

For a sharp, smooth film with $\phi_t = 0$, the final reflectance maximum occurs just as film removal is completed. With a transition region, f and ϕ_t are constant if this region maintains fixed size and shape, but are expected to vary once the region begins to collapse into the substrate near the endpoint of film removal. An observable effect of f and ϕ_t varying is the end-point according to the laser interferogram occurring slightly before the

final extrapolated reflectance maximum. The shape of the R versus time curve near the endpoint can provide clues to the shape of the concentration profile through the transition region (see figure 2). In RIE, film roughening is expected from ion bombardment of the exposed surface. Roughening of the 1-2 interface can produce an amplitude reduction in reflectance oscillations similar to that due to diffuseness if the laser beam is sufficiently wide compared to the roughness correlation length. But scattering from the rough interface also deflects energy out of the specular directions and introduces additional corrections into R. As a first approximation, these corrections can be neglected and the interferometer waveform for RIE analyzed using a modified version of diffuse interface transition layer theory.

When $|r_{12}| \ll 1$, as for most polymer films dissolving in solvents, R is well-approximated by a power series in r_{12} to first order:

$$R = r_{23}^2 + 2fr_{12}r_{23}(1-r_{23}^2)\cos\phi \qquad (3)$$

Physically, this amounts to considering emerging rays whose histories involve no more than one reflection from the 1-2 interface. R is then a purely sinusoidal function of ϕ (and of film thickness d), oscillating about the value $R_o = r_{23}^2$. The factor f reduces the oscillation amplitude symmetrically about $R = R_o$ which facilitates straightforward calculation of polymer refractive index from quantities measured directly from the waveform [3]. When $|r_{12}|$ is not small, as in the plasma etching of thin polymer films, the first order power series approximation is inadequate. For example, for a plasma/poly(methylmethacrylate)/silicon system, $r_{12} = -0.196$ and $r_{23} = -0.442$. The waveform for a uniformly etching film is no longer purely sinusoidal in time but contains other harmonic components. In addition, amplitude reduction

through the f factor does not preserve the vertical median R_o making the film refractive index calculation non-trivial.

Figure 3 is a sketch of a typical waveform obtained during an oxygen/RIE process. Referring to this figure, let $R_\pm$ be the extreme values of R when the transition layer is present. Let $R^o_\pm$ be the corresponding values if the interface were sharp (f=1). These values can be identified by setting $\cos\phi = \pm 1$ in equation (1) which gives,

$$R_\pm = \left(\frac{r_{23} \pm f r_{12}}{1 \pm f r_{12} r_{23}} \right)^2 \qquad (4)$$

$$R^o_\pm = \left(\frac{r_{23} \pm r_{12}}{1 \pm r_{12} r_{23}} \right)^2 \qquad (5)$$

Remember that $R^o_+ = r^2_{13}$, the reflectance of the bare substrate medium. As before, let R_o be the value of R for which $\cos\phi=0$ in (1),

$$R_o = \left(\frac{r^2_{23} + f^2 r^2_{12}}{1 + f^2 r^2_{12} r^2_{23}} \right) \qquad (6)$$

Note that the points on the waveform for which $R=R_o$ are equally spaced along ϕ for a uniformly decreasing film thickness, thus making them identifiable. The plasma itself contributes to the measured intensity. This contribution, defined as R_p, must be subtracted from the reflectance values before any calculations are made. R_p is measured by extinguishing the plasma and measuring the corresponding reduction in intensity. No evidence of non-linear optical effects are observed.

When f=1, the directly measurable ratio $x^o = (R^o_-/R^o_+)^{\frac{1}{2}}$ for normal or near normal incidence can be easily used to determine n_2, knowing n_1 and n_3. At normal incidence,

$$R_+^o = \left(\frac{n_3 - n_1}{n_3 + n_1} \right)^2 \tag{7a}$$

$$R_-^o = \left(\frac{n_3 n_1 - n_2^2}{n_3 n_1 + n_2^2} \right)^2 \tag{7b}$$

Solving for n_2 in terms of x^o yields,

$$n_2 = (n_3 n_1)^{\frac{1}{2}} \left[\frac{\left(\frac{n_3 + n_1}{n_3 - n_1} \right) - x^o}{\left(\frac{n_3 + n_1}{n_3 - n_1} \right) + x^o} \right]^{\frac{1}{2}} \tag{8}$$

For unpolarized light, this relation is a very good approximation for incidence angles $\vartheta_1 \leq 15°$. When f<1, the observed ratio is $x = (R_-/R_+)^{\frac{1}{2}} < x^o$. If r_{12} were small, then the fact that f would compress the waveform symmetrically about the value R_o could be used to find x^o, and hence n_2. Note that this analysis would also immediately determine f because equation (3) would apply, and f would be the amplitude reduction factor for the reflectance oscillations. But if r_{12} is not small, then a more careful analysis is needed.

Consider the quantities $\Delta R_\pm^{\frac{1}{2}} = |R_\pm^{\frac{1}{2}} - R_\pm^{o\frac{1}{2}}|$, which denote the shifts in the extreme values of $R^{\frac{1}{2}}$ due to spreading of the interface. Using equations (4) and (5), these can be written as

$$\Delta R_\pm^{\frac{1}{2}} = \left| \frac{(1 - f) r_{12} (1 - r_{23}^2)}{(1 \pm f r_{12} r_{23})(1 \pm r_{12} r_{23})} \right| \tag{9}$$

One then finds

$$\left(\frac{\Delta R_-^{\frac{1}{2}}}{\Delta R_+^{\frac{1}{2}}} \right) = \left(\frac{1 + f r_{12} r_{23}}{1 - f r_{12} r_{23}} \right) \left(\frac{1 + r_{12} r_{23}}{1 - r_{12} r_{23}} \right) \tag{10}$$

If the right side of equation (10) were known or could be estimated reasonably well, the equation could then be used to find R_-^o from normalized values of R_+, R_+^o, and R_-, which are available experimentally. If (1 - f) were small, then the fractional shifts $\Delta R_\pm / R_\pm^o$ would also be small, and vice-versa, so that the ratio of shifts could be written via differentials as

$$\left(\frac{\Delta R_-}{\Delta R_+} \right) \approx \left(\frac{R_-}{R_+} \right)^{\frac{1}{2}} \left(\frac{\Delta R_-^{\frac{1}{2}}}{\Delta R_+^{\frac{1}{2}}} \right) \tag{11}$$

But the right side of equation (10) is not known <u>a priori</u>. A crude approximation might be to set it equal to unity, and equation (11) would then give

$$(\Delta R_-/\Delta R_+) \approx (R_-/R_+)^{\frac{1}{2}} = x \tag{12}$$

This crude approximation gives a rather simple result but is probably not accurate enough for most purposes. However, it turns out that the quantities on the right side of (10) can be obtained from a more careful analysis of the interferometer waveform. And once these quantities are known, n_2 can then be found directly from them without recourse to equations (11) or (12).

Consider the general form of the reflectance R from equation (1), namely

$$R = \left(\frac{a + c(\cos\phi)}{b + c(\cos\phi)} \right) \tag{13}$$

where

$$a = r_{23}^2 + f^2 r_{12}^2 \tag{14a}$$

$$b = 1 + f^2 r_{12}^2 r_{23}^2 \tag{14b}$$

$$c = |2f r_{12} r_{23}| \tag{14c}$$

In terms of these one can write previously defined quantities as

$$R_{\pm} = \left(\frac{a \pm c}{b \pm c}\right) \tag{15}$$

$$R_o = a/b \tag{16}$$

Now define the directly measurable ratios

$$Q_{\pm} \equiv R_{\pm}/R_o = \left(\frac{1 \pm c/a}{1 \pm c/b}\right) \tag{17}$$

Letting A=a/c and B=b/c, and solving equations (17) for A and B, one obtains

$$A = \left(\frac{Q_+ - Q_-}{Q_+ + Q_- - 2Q_+Q_-}\right) \tag{18a}$$

$$B = \left(\frac{Q_+ - Q_-}{2 - Q_+ - Q_-}\right) \tag{18b}$$

Letting $y = |fr_{12}/r_{23}|$ and $z = |fr_{12}r_{23}|$, one finds that $2A = y + 1/y$ and $2B = z + 1/z$, from which y and z are found to be

$$y = |A - (A^2 - 1)^{\frac{1}{2}}| \tag{19a}$$

$$z = |B - (B^2 - 1)^{\frac{1}{2}}| \tag{19b}$$

Equation (19b) is valid in general, whereas (19a) holds only if $y \leq 1$, a condition which in practice can be arranged. However, if it happens to be known that $y > 1$, then the opposite sign preceding the square root term in (19a) should be used. Once A and B are known, it follows that

$$|fr_{12}| = (zy)^{\frac{1}{2}} \tag{20a}$$

$$|r_{23}| = (z/y)^{\frac{1}{2}} \tag{20b}$$

Now the task is to determine f.

First define the directly measurable quantity $w = (R_+/R_+^o)^{\frac{1}{2}}$. Using equations (4), (5), and (20), w can be written in terms of y, z, and f as

$$w = \left(\frac{(1 + y)(1 + z/f)}{(1 + z)(1 + y/f)} \right) \tag{21}$$

which can then be solved for f to give

$$f = \left(\frac{y - z - y(1 + z)(1 - w)}{y - z + (1 + z)(1 - w)} \right) \tag{22}$$

Equations (21) and (22) involve the assumption that r_{12} and r_{23} are both of the same algebraic sign, so that either $n_1 < n_2 < n_3$ or $n_3 < n_2 < n_1$. Otherwise, appropriate sign adjustments must be made. Knowing f and $|fr_{12}|$, one may then determine $|r_{12}|$.

Finally, assuming that $n_1 < n_2 < n_3$, a condition typical in RIE, one notes that

$$|r_{12}| = \left(\frac{n_2 - n_1}{n_2 + n_1} \right) \tag{23a}$$

$$|r_{23}| = \left(\frac{n_3 - n_2}{n_3 + n_2} \right) \tag{23b}$$

which leaves two ways to solve for the polymer refractive index, n_2,

$$n_2 = \left(\frac{1 + |r_{12}|}{1 - |r_{12}|} \right) n_1 \tag{24a}$$

$$n_2 = \left(\frac{1 - |r_{23}|}{1 + |r_{23}|} \right) n_3 \tag{24b}$$

A local etch rate can be calculated once n_2 is determined. The change in thickness corresponding to one complete oscillation is known as the thickness period, d_p,

$$d_p = \frac{\lambda}{2\,[n_2^2 - n_1^2 \sin^2\theta_1]^{\frac{1}{2}}} \tag{25}$$

which is constant as long as the film properties are not changing during the process. The local etch rate is related to d_p and the temporal period of oscillation, T (see figure 3),

$$\text{etch rate} = d_p/T \tag{26}$$

EXPERIMENTAL

All waveforms were collected using a reactive-ion etcher built in-house equipped with a He-Ne laser (λ=632.8nm) interferometer as depicted in figure 4. The laser beam was aimed at the substrate surface at an angle of 10° relative to the normal. Laser intensity was measured by a photodiode whose signal was passed through a transimpedance amplifier/low pass filter (cutoff frequency = 10Hz) circuit and digitally recorded by an IBM personal computer. Dry oxygen was used exclusively as the etch gas. Films of poly(methylmethacrylate), PMMA (KTI Chemicals,950k), and VMCH, a commercially available poly(vinylchloride-vinyl acetate-maleic anhydride) terpolymer were spun from 6% solutions in chlorobenzene onto 3" silicon wafers at 1500 rpm and pre-baked at 160°C for 1 hour yielding film thicknesses of 1μm ± 0.1.

Surface roughness was measured according to ANSI standard 1346.1-(1978) using a Tencor Instruments Alpha-Step 200 stylus profilometer located at the National Nanofabrication Facility of Cornell. Five surface roughness measurements were made for each sample and their average values recorded. Details of the experimental apparatus set-up and its operation are given elsewhere [4].

DATA ANALYSIS

The interferometric data were digitally smoothed (attenuation range = 0.9995-1.005) and differentiated so that the local minima (=R_-) and maxima (=R_+) of the interferogram could be located and averaged over a given run. An average value of the medium/substrate reflectance, R_+^o (=r_{13}^2), was also calculated over a ten second period after the end-point had been reached. The plasma intensity was then determined by extinguishing the plasma. The baseline measurement for the background intensity was measured by closing the shutter on the laser for about five seconds immediately before each run. Initial results showed that it was very difficult to determine R_o experimentally due to small increases (≈5%/min.) in etch rate with time. Therefore, an initial guess of $R_o = \frac{1}{2}(R_+ + R_-)$ was used. These values were input to a computer program which computed the polymer's refractive index (=n_2) by the following iterative scheme.

After subtracting the baseline and plasma intensity, experimental R_-, R_+, R_+^o, and R_o values were substituted in equations (17)-(20) and (22) and solved for $|r_{12}|$ and $|r_{23}|$. The polymer refractive index was then calculated with equations (24a) and (24b) and the results between the two compared. The value of R_o was then appropriately adjusted and the process repeated using the new R_o until the n_2-values calculated by equations (24a) and (24b) agreed to within 0.1%. Singularities in the expressions for parameters A and B in equations (18a) and (18b) were avoided by making a 5% change in R_o when necessary. Convergence was usually achieved in less than ten iterations.

RESULTS

Results of refractive index measurements for PMMA and VMCH during oxygen RIE at 35mTorr and various incident rf power densities are tabulated in Table 1. The values in the first column are those obtained using the full reflectance relation (1) while those in the second column were calculated assuming $r_{12}<<1$. The calculated n_2 values are invariant with respect to power level to within experimental error. The more rigorous analysis makes a 2-4 percent correction to the $r_{12}<<1$ case and yields results that are in good agreement with values cited in the literature or measured by other methods.

The laser interferometer appears to be sensitive enough to detect small changes in surface structure. Figure 5 is a plot of amplitude reduction factor versus incident power density obtained for PMMA and VMCH films at 35mTorr. It is seen that f decreases with rf power which may indicate that more surface roughening occurs at higher ion bombardment energies. Extrapolation of the curves to zero power does not necessarily go through f=1 (i.e. sharp interface), particularly for the PMMA curve. This is consistent with the fact that scattering of light by pre-etched PMMA films was always observed during the experiments whereas scattering by pre-etched (post-bake) VMCH films, while present to a small extent, was noticeably less. Roughness amplitudes estimated from f using transition layer theory [3] range from 60 to 130 Å for PMMA and from 80 to 140 Å for VMCH.

Table 2 summarizes surface roughness values measured for PMMA and VMCH samples etched for 1.0 minute at 35mTorr at various power densities. Although the measured values of 80 - 105 Å fall within the ranges obtained from the interferometer and transition layer theory, there is no significant variation

with power density. Differences in surface roughness between pre-etched films of PMMA and VMCH are also negligible according to the stylus measurements.

Table 3 is a summary of results obtained for O_2/RIE of PMMA at 0.125 Watts/cm^2 and 0.75 Watts/cm^2 and 5mTorr and 35mTorr. The amplitude reduction factor is approximately equal to unity (sharp/smooth surface) at 5mTorr for both power levels while measured differences exist at 35mTorr. The etch rates are 2-3 times lower at 5mTorr than the corresponding rates at 35mTorr. In addition, the dark space width, measured with a cathetometer, increased from 1.1cm at 35mTorr to 3.0cm at 5mTorr while self-bias potentials were only modestly higher at 5mTorr. Non-local transport theories [5] predict comparable energy deposition rates at these conditions but ion fluxes that are two to six times greater at 35mTorr than at 5mTorr. Apparently, surface roughness and etch rate scale with ion flux to the surface.

SEM photomicrographs of etched films confirm these findings. Figures (6a)-(6c) are SEM photomicrographs taken of PMMA films etched for one minute under the following O_2/RIE conditions: (6a) baked/unetched, (6b) 0.125 Watts/cm^2, 35mTorr; (6c) 0.75 Watts/cm^2, 35mTorr. It is clear that the film surfaces etched at 35mTorr become progressively rougher with increasing power density. Similar SEM analyses showed the films etched at 5mTorr to remain smooth after identical etching intervals. The characteristic wavelength of the corrugated surface folds of the roughened films appear to increase from less than 0.1μm at low power to about 0.2μm at high power. These wavelengths are less than wavelength of the probing laser beam and insure that the beam is indeed optically averaging the surface roughness. Had the surface corrugations been of sufficiently long wavelength, then the reflected beam signal would carry

only local information about the film surface and would make the results difficult to interpret.

In these oxygen/RIE experiments, the effect of the transition layer phase shift ϕ_t is such that the endpoint begins close to the final extrapolated reflectance maximum, perhaps anticipating it slightly as expected for a rough film (figure 7). The approach to completion of etch removal appears to be more gradual than is ordinarily seen in film dissolution experiments, with no evidence of acceleration or steep inflection in the concentration profile within the transition region. The concentration profile for a simple rough interface is not expected to show any sharp inflection unless some intrinsic layering structure (i.e. residual etch products) were present, and none is evident from the interferogram. Furthermore, there is no reason to expect acceleration of etch removal near the endpoint since etch rate is limited by generation of active etchant species (atomic oxygen and O_2^+ ions) in the gas phase [6-9]. The observations are consistent with this expectation.

DISCUSSION

Refractive index measurements made by this technique are of sufficient accuracy to make this a valuable research tool in studying and characterizing the dry etch behavior of novel polymer resist materials. *In situ* etch rate can be measured and analyzed quickly without any prior knowledge of the polymer's physical properties.

Surface "roughness" measurements of reactive-ion etched samples suggest that laser interferometry may be more sensitive than mechanical stylus measurements. This apparent difference in sensitivity is due to the fact that surface roughness correlation lengths in this study are

less than 0.2μm. This is less than laser beam's wavelength which insures that the probing beam is optically averaging the surface roughness and makes it intrinsically sensitive enough to use as a RIE characterization tool. On the other hand, surface roughness magnitudes of this order are beyond the sensitivity of a 5-12μm diameter mechanical stylus tip. Similar conclusions were drawn in the ellipsometric surface study by Nee [10].

The key factor in obtaining precise information from the oxygen/RIE laser interferogram is careful process control which minimizes signal noise. The calculations are very sensitive to small changes in reflected beam signal. In many cases, the amplitudes of waveform oscillations can vary by a few percent during a run which can lead to proportionate changes in calculated n_2 and f values. Estimates of the plasma intensity, R_p, are a function of the time at which it is measured and the surface area of exposed etchable material during the process. The plasma intensity is typically a few percent greater during the etch when etchable material is still present. This was confirmed by measuring the plasma intensity periodically throughout an etch cycle.

CONCLUSIONS

The full expression for the reflected intensity of a laser interferometer in a plasma/polymer/silicon system can be used to measure the polymer refractive index to within about 3 percent. This leads to an efficient and non-destructive *in situ* etch rate measurement technique which does not require any prior knowledge of film properties. The analysis can also be used to gauge the degree of "roughening" imparted to a polymer film surface in a plasma etching environment in a semi-quantitative manner.

REFERENCES

1. P.D. Krasicky, R.J. Groele, and F. Rodriguez, Chem. Eng. Comm., 54, 279, (1987).

2. A. Vasicek, "Optics of Thin Films", North-Holland Pub., Ambsterdam, (1960).

3. P.D. Krasicky, R.J. Groele, and F. Rodriguez, J.Appl.Polymer Science, 35, 641, (1988).

4. B.C. Dems, F.Rodriguez, C.M. Solbrig, Y.M.N. Namaste, and S.K. Obendorf, Intl. Polym. Proc., (to be published).

5. C.W. Jurgensen, J. Appl. Phys., 64(2), 590, (1988).

6. J.F. Battey, IEEE Trans. on Elec. Dev., 24(2), 140, (1977).

7. M.A. Hartney, W.M. Greene, D.S. Soane, and D.W. Hess, SPIE Proceedings - Adv. in Resist Tech. and Proc. V, Vol.920, 108, (1988).

8. H. Gokan and S. Esho, J. Electrochem. Soc., 131, 1106, (1984).

9. B.R. Soller and R.F. Shuman, J. Electrochem. Soc., 131, 1353, (1984).

10. S.F. Nee, Applied Optics, Vol.27, No.14, 2819, (1988).

TABLE 1

Calculation of Polymer Refractive Index from Laser Interferometer Waveform during Oxygen RIE*

POWER DENSITY (Watts/cm^2)	SELF-BIAS (-VDC)	PMMA		VMCH	
		$r_{12}=r_{23}$	$r_{12}<<r_{23}$	$r_{12}=r_{23}$	$r_{12}<<r_{23}$
0.125	250	1.461	1.444	1.508	1.481
0.25	350	1.481	1.442	1.512	1.462
0.50	450	1.482	1.446	1.501	1.456
0.75	520	1.466	1.435	1.528	1.484
0.875	550	1.486	1.444	1.511	1.454
Accepted value		1.489		1.535**	
Standard deviation of measurement		±0.010		±0.011	

* RIE conditions: Flow=20 SCCM O_2, pressure=35mTorr
** Measured experimentally with Rudolph Instruments ellipsometer

TABLE 2

Average Surface Roughness of Etched PMMA and VMCH Films

POWER DENSITY (Watts/cm^2)	SELF-BIAS (-VDC)	SURFACE ROUGHNESS* (Å) PMMA	VMCH
unetched		40	35
0.125	250	100	85
0.25	350	90	95
0.50	450	80	105
0.75	520	90	80
1.05	575	85	90

* Surface Roughness measured with Tencor Instruments Alpha-Step 200 stylus profilometer per ANSI Standard 1346.1-(1978)

O_2/RIE Conditions: flow=20 SCCM, chamber pressure=35mTorr
Etch time = 1.0 minute

TABLE 3

Amplitude Reduction Factor and Oxygen RIE Rate of PMMA

Power Density (Watts/cm^2)	Pressure (mTorr)	Self-Bias (-VDC)	f	Etch Rate* (nm/min)
0.125	5	250	0.993	135
0.750	5	600	0.999	435
0.125	35	230	0.966	245
0.750	35	500	0.945	1160

* Time-weighted average

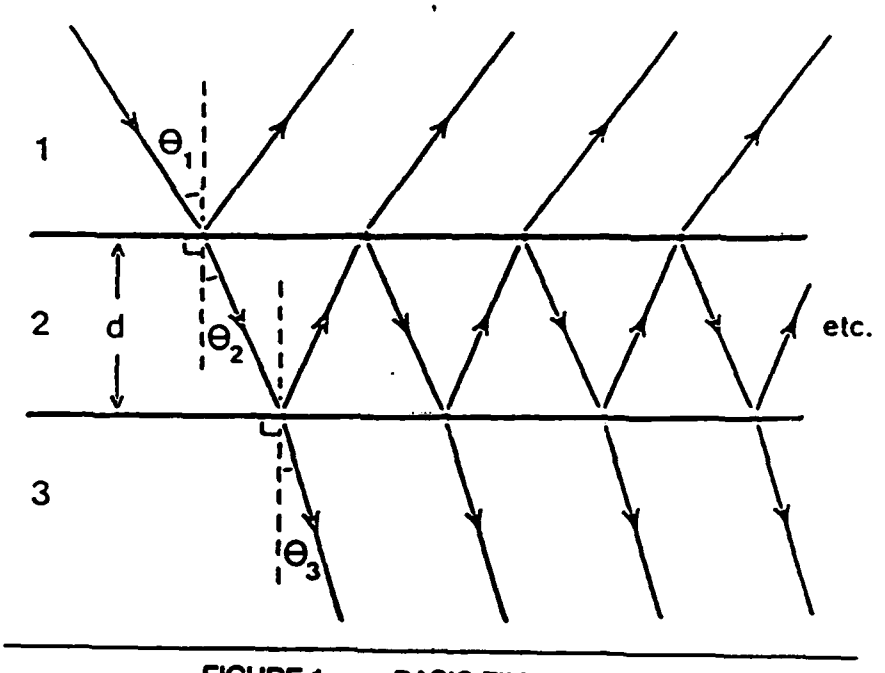

FIGURE 1: BASIC FILM MODEL

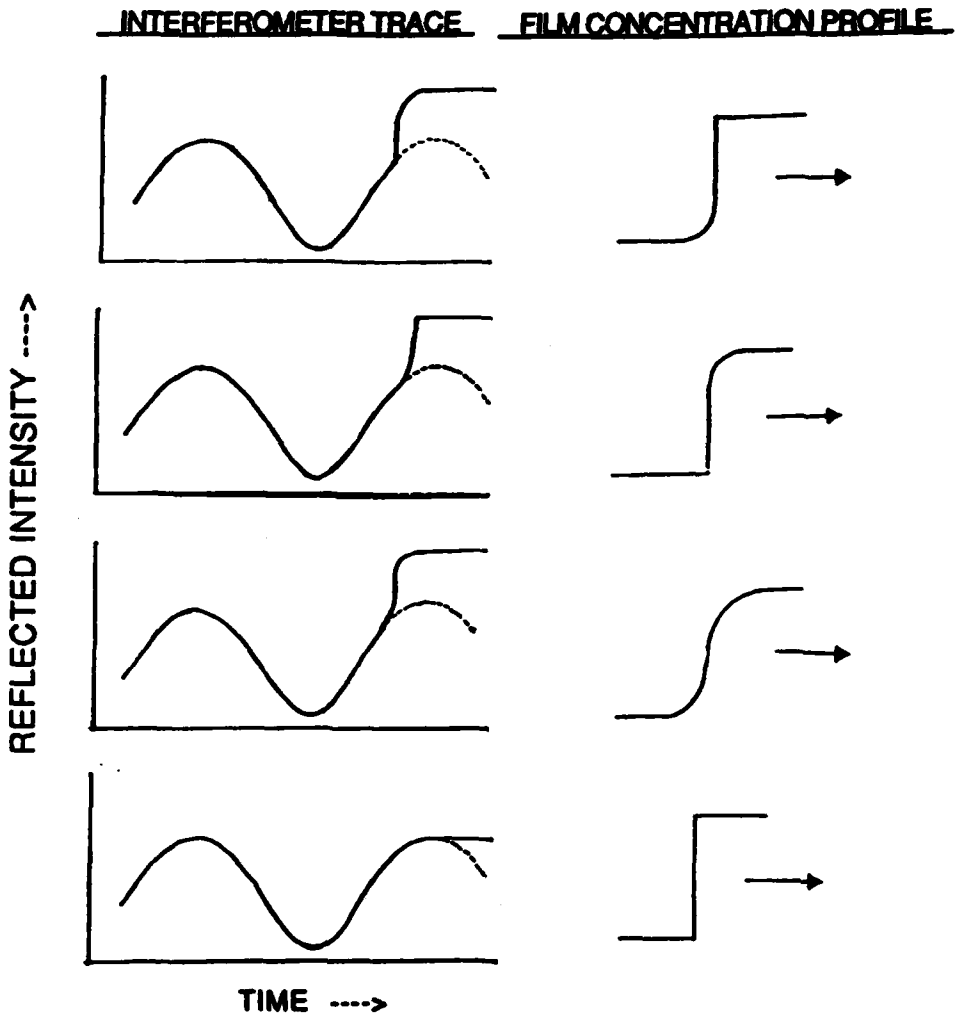

FIGURE 2: WAVEFORM DEPENDENCE ON CONCENTRATION PROFILE NEAR THE END-POINT

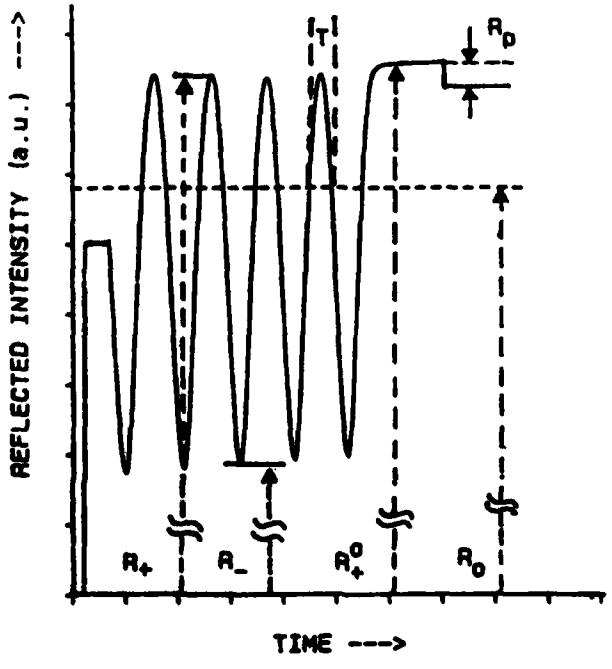

FIGURE 3: TYPICAL OXYGEN RIE INTERFEROGRAM

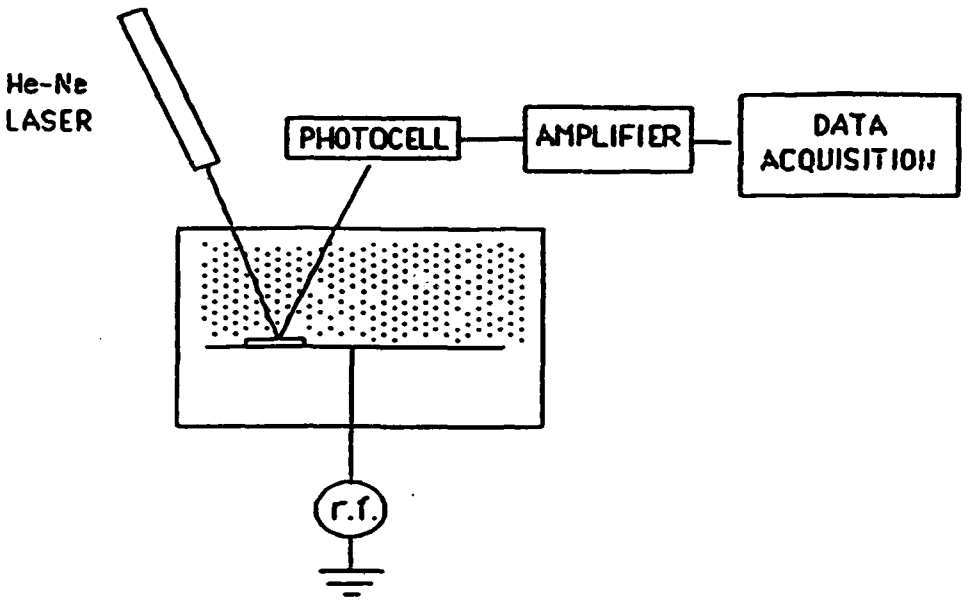

FIGURE 4: RIE/LASER INTERFEROMETER

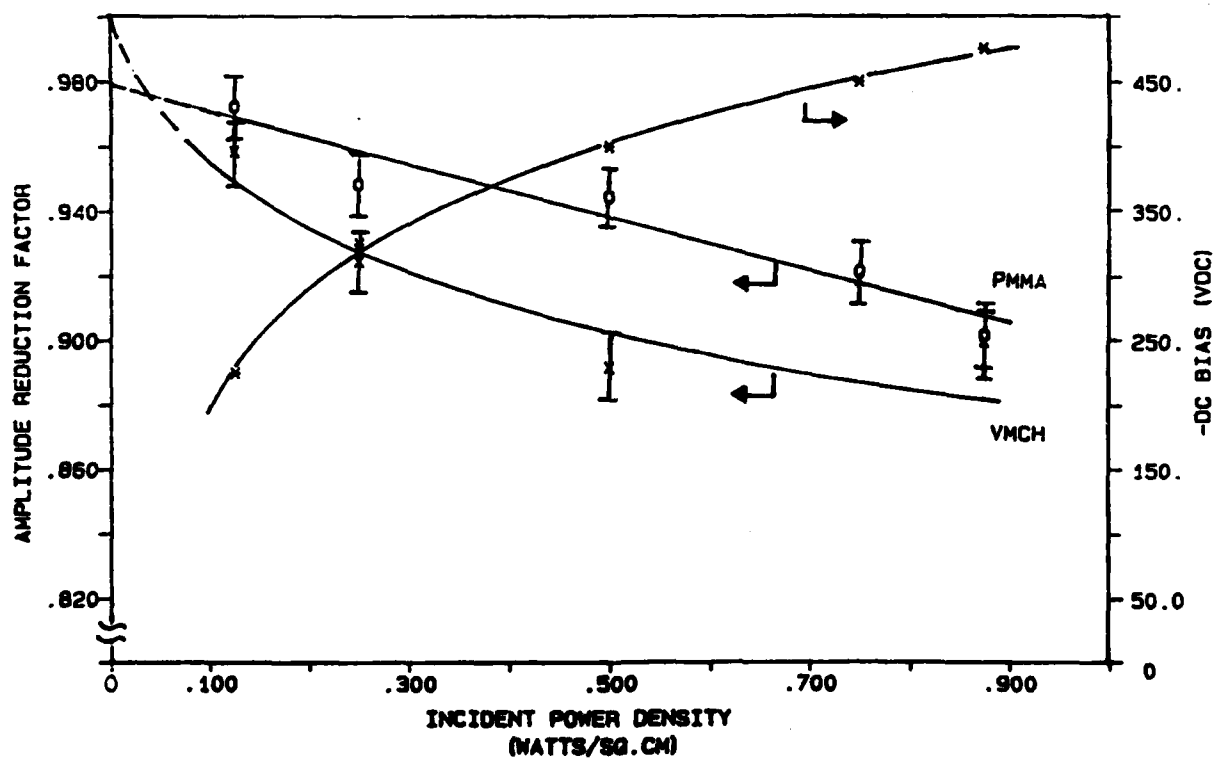

FIGURE 5: AMPLITUDE REDUCTION FACTOR AND SELF-BIAS POTENTIAL VERSUS POWER DENSITY AT 35mTORR

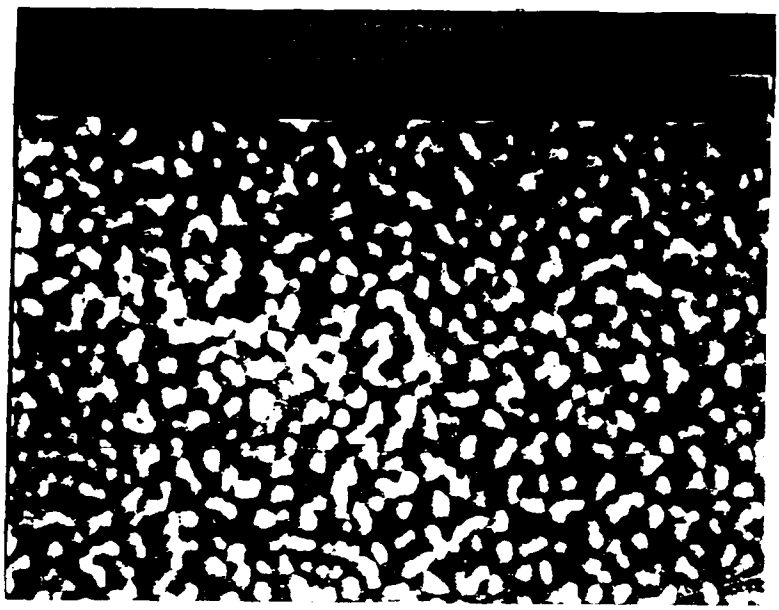

DL/1113/89/1

TECHNICAL REPORT DISTRIBUTION LIST, GENERAL

	No. Copies
Office of Naval Research Chemistry Division, Code 1113 800 North Quincy Street Arlington, VA 22217-5000	3
Commanding Officer Naval Weapons Support Center Attn: Dr. Bernard E. Douda Crane, IN 47522-5050	1
Dr. Richard W. Drisko Naval Civil Engineering Laboratory Code L52 Port Hueneme, California 93043	1
Defense Technical Information Center Building 5, Cameron Station Alexandria, Virginia 22314	2 high quality
David Taylor Research Center Dr. Eugene C. Fischer Annapolis, MD 21402-5067	1
Dr. James S. Murday Chemistry Division, Code 6100 Naval Research Laboratory Washington, D.C. 20375-5000	1
Dr. Ronald L. Atkins Chemistry Division (Code 385) Naval Weapons Center China Lake, CA 93555-6001	1
Chief of Naval Research Special Assistant for Marine Corps Matters Code 00MC 800 North Quincy Street Arlington, VA 22217-5000	1
Dr. Bernadette Eichinger Naval Ship Systems Engineering Station Code 053 Philadelphia Naval Base Philadelphia, PA 19112	1
Dr. Sachio Yamamoto Naval Ocean Systems Center Code 52 San Diego, CA 92152-5000	1
David Taylor Research Center Dr. Harold H. Singerman Annapolis, MD 21402-5067 ATTN: Code 283	1